FULL PAPER

Injectable Stem Cell-Laden Photocrosslinkable Microspheres Fabricated Using Microfluidics for Rapid Generation of Osteogenic Tissue Constructs

Xin Zhao, Shen Liu, Lara Yildirimer, Hong Zhao, Ruihua Ding, Huanan Wang, Wenguo Cui,* and David Weitz*

Direct injection is a minimally invasive method of stem cell transplantation for numerous injuries and diseases. However, despite its promising potential, its clinical translation is difficult due to the low cell retention and engraftment after injection. With high versatility, high-resolution control and injectability, microfabrication of stem-cell laden biomedical hydrogels holds great potential as minimally invasive technology. Herein, a strategy of microfluidics-assisted technology entrapping bone marrow-derived mesenchymal stem cells (BMSCs) and growth factors in photocrosslinkable gelatin (GelMA) microspheres to ultimately generate injectable osteogenic tissue constructs is presented. Additionally, it is demonstrated that the GelMA microspheres can sustain stem cell viability, support cell spreading inside the microspheres and migration from the interior to the surface as well as enhance cell proliferation. This finding shows that encapsulated cells have the potential to directly and actively participate in the regeneration process. Furthermore, it is found that BMSCs encapsulated in GelMA microspheres show enhanced osteogenesis in vitro and in vivo, associated with a significant increase in mineralization. In short, the proposed strategy can be utilized to facilitate bone regeneration with minimum invasiveness, and can potentially be applied along with other matrices for extended applications.

1. Introduction

Stem cell transplantation has emerged as a promising therapeutic strategy for the treatment of various injuries ranging from bony fractures to bone cancers and for other disorders.[1] Amongst the plethora of stem cells, bone marrow-derived mesenchymal stem cells (BMSCs) are frequently used for bone regeneration due to their osteogenic differentiation potential.[2] Direct injection of cells into the repair site minimizes surgical invasiveness and is thus gaining in popularity for clinical applications.[3] However, low retention and low engraftment of directly injected cells still represent major hurdles for successful clinical translation.[3] Low cell retention may be caused by mechanical shear forces that damage cell membrane during the injection or by a lack of 3D structure to enhance the engraftment, viability, and function of the injected cells.[4] Indeed, the lack of suitable cellular delivery vehicles

Dr. X. Zhao, H. Zhao, R. Ding, Dr. H. Wang, Prof. W. Cui, Prof. D. Weitz
John A. Paulson School of Engineering and Applied Sciences
Harvard University
Cambridge, MA 02138, USA
E-mail: wgcui80@hotmail.com; weitz@seas.harvard.edu

Prof. D. Weitz
Department of Physics
Harvard University
Cambridge, MA 02138, USA

Dr. X. Zhao
The Key Laboratory of Biomedical Information Engineering of Ministry of Education
School of Life Science and Technology
Xi'an Jiaotong University
Xi'an 710049, Shanxi, China

Dr. X. Zhao
Bioinspired Engineering and Biomechanics Center
Xi'an Jiaotong University
Xi'an 710049, China

Dr. S. Liu
Department of Orthopaedic Surgery
Shanghai Sixth People's Hospital Affiliated to Shanghai Jiaotong University
Shanghai 200233, China

Dr. L. Yildirimer
Centre for Nanotechnology and Regenerative Medicine
UCL Division of Surgery and Interventional Science
University College London
London WC1E 6AU, UK

Prof. W. Cui
Department of Orthopedics, the First Affiliated Hospital of Soochow University
Orthopedic Institute
Soochow University
708 Renmin Road, Suzhou, Jiangsu 215006, China

FULL PAPER

currently limits the successful application of injectable BMSC-based therapies for bone regeneration.

One potential attractive strategy for stem cell delivery that overcomes these limitations is to suspend the stem cells in hydrogels which can be injected and solidified *in situ*. Hydrogels have a high water content, similar to tissues, which not only enables homogeneous encapsulation of cells and growth factors, but also allows for facile delivery via injection. Their readily tunable degradation properties provide further control over the release behavior of incorporated cargo material.[5] Hydrogels of synthetic origin, poly (ethylene glycol) diacrylate (PEGDA),[6] and of natural origin, such as hyaluronic acid (HA),[7] alginate,[8] collagen,[9] and gelatin[10] have been tested. However, their clinical success has frequently been impeded by insufficient oxygen and nutrient supply due to the large size of the bone defects, which compromises cell survival and performance, resulting in poor bone regeneration.[11] Furthermore, the bulk environment and the limited interfacial interactions between the cells and the hydrogel material restrict tissue regeneration. Therefore, development of alternate hydrogel geometries for stem cell delivery is required to further drive clinical translation of BMSC-based bone repair strategies.

One such geometry is hydrogel microspheres which can encapsulate both stem cells and their growth factors; they facilitate nutrient and waste transfer and thereby maintain the viability of preseeded cells, while also preserving the scaffold's injectability.[12,13] In addition, such 3D scaffolds have large surface area which improves cell-matrix interactions. Thus the use of hydrogel microspheres to encapsulate the stem cells has great potential for tissue regeneration.[14,15] Hydrogel microspheres of suitably large size can be conveniently generated using a microfluidic approach which allows one-step fabrication of monodisperse microspheres of controlled sizes with high cell encapsulation efficiency and high cell survival rate.[16] The most commonly used materials to fabricate these microspheres are PEGDA[17] and sodium alginate.[13,15] However, these carriers lack cell-responsive anchorage points, which greatly limits cell proliferation, elongation, migration and organization into higher order structures, and therefore they are not conducive to osteogenic differentiation.[15,18] Additionally, neither the PEGDA nor the alginate systems are degradable by cells, limiting the cell motion within the 3D microenvironment.[19] An alternative material with which to fabricate these microspheres is natural extracellular matrix (ECM) protein such as collagen or its denatured form, gelatin. These contain bioactive and cell adhesive sequences that support cell attachment and proliferation, while also promoting osteogenic differentiation.[20] Nevertheless, self-assembled collagen or gelatin microspheres are difficult to fabricate due to their poor mechanical stability.[9,21] Crosslinking collagen or gelatin microspheres using agents such as glutaraldehyde,[22] carbodiimides,[23] genipin,[24] or transglutaminase (mTG)[25] results in cytotoxicity and immunogenicity,[26] rendering these agents ill-suited for creating cell-laden microspheres. Furthermore, these crosslinking methods usually require several hours to achieve mechanical stability, which limits their clinical applicability particularly for repair of acute bone defects. Thus, the use of stem-cell laden hydrogel microspheres for bone regeneration has been limited.

In the present study, a microfluidic approach to rapidly generate hydrogel microspheres that encapsulate bone-marrow-derived stem cells and growth factors and create a favorable cell growth microenvironment that enhances osteogenesis is presented. Droplets of photocrosslinkable gelatin, gelatin methacryloyl (GelMA), containing photoinitiator (PI) are produced in a microfluidic device and are subsequently photopolymerized to quickly and efficiently generate GelMA microspheres. This gentle gelling condition minimizes damage to the incorporated cells and proteins. It is demonstrated that the GelMA microspheres enhance cell proliferation, offer controlled release of growth factors and the encapsulated BMSCs exhibit significant osteogenesis both in vitro and in vivo. Furthermore, the GelMA microspheres are capable of not only supporting cell viability and spreading within the microspheres, but also cell migration from the interior outwards to the microsphere surface.

2. Results and Discussion

2.1. Overview

A schematic overview of the experiments reported in the paper is shown in **Figure 1**. The GelMA hydrogel microspheres were fabricated with a flow-focusing capillary microfluidic device that produces aqueous drops of the precursor polymers in carrier oil. The drops were exposed to UV radiation to initiate gelation, resulting in BMSC-laden hydrogel microspheres that were approximately 160 μm in diameter. These were then removed from the carrier oil and suspended in cell medium. The osteogenic potential of the BMSCs was measured both in vitro and in vivo, with the latter tests being conducted using a rabbit femoral condyle model.

2.2. Microfluidic Fabrication of GelMA Microspheres

Photocrosslinkable gelatin (GelMA) was synthesized by substituting amines in gelatin with methacrylamide.[27] The degree of substitution of GelMA was determined by ^{1}H nuclear magnetic resonance spectroscopy (NMR). Based on the ^{1}H NMR analysis, the synthesized GelMA displayed a high degree of methacrylation, 75% (Figure S1, Supporting Information). Spherical BMSC-laden GelMA microspheres were fabricated using a microfluidic flow-focusing device (**Figure 2**A). Such approach was particularly suitable for rapid and high-throughput production of hydrogel microspheres that were both highly monodisperse in size and sufficiently large for the intended purpose.[28] Aqueous GelMA droplets were formed as a water in oil emulsion (Figure 2B). The aqueous phase consisted of 7.5 wt% GelMA and 1.0 wt% photoinitiator which enabled photopolymerization and formation of spherical hydrogel microdroplets. The GelMA concentration was chosen to be above the lower critical concentration for hydrogel formation of 4.0 wt% and below a concentration of 8.0 wt%, which was found to impede cell spreading within the microspheres. The oil phase consisted of perfluorinated oil (3M HFE 7500). The drops were stabilized by a biocompatible triblock perfluorinated copolymer surfactant (1.0 wt%, Krytox-PEG, RAN Biotech).[29]

www.MaterialsViews.com

ADVANCED
FUNCTIONAL
MATERIALS
www.afm-journal.de

FULL PAPER
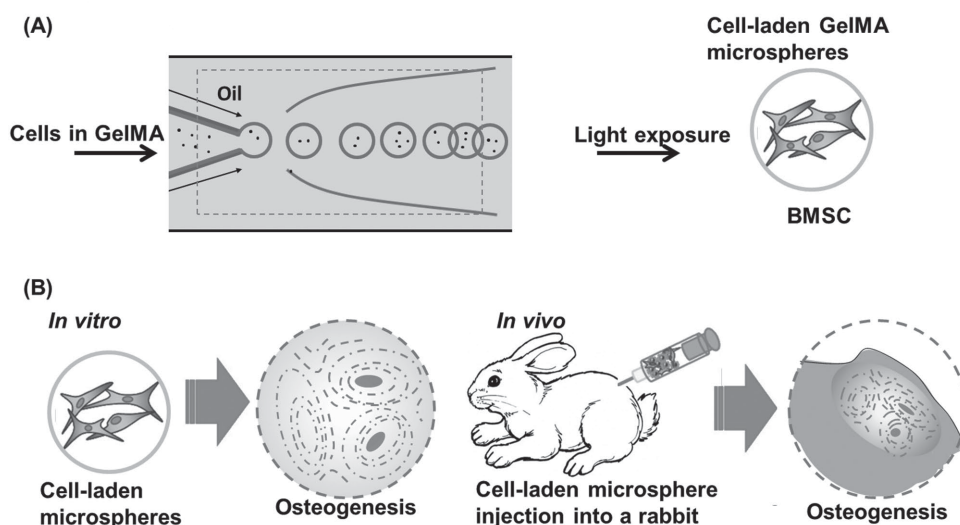
Figure 1. Schematic diagram of fabrication of BMSC-laden GelMA microspheres and its application for osteogenesis and regeneration of injured bones. A) Photocrosslinking-microfluidic fabrication of GelMA microspheres. Aqueous droplets containing GelMA gel precursors are produced from a microfluidic flow-focusing device and photopolymerized to form GelMA microspheres. B) Osteogenesis of BMSC embedded in GelMA microspheres. BMSCs encapsulated in GelMA microspheres differentiate and regenerate bone in vitro and in vivo.

A capillary microfluidic flow-focusing device was used in the present study due to its superiority over conventional emulsification techniques which use mechanical agitation such as sonication. The microfluidic device produced droplets of high monodispersity and controllable size.[30] Flow rates of the GelMA solution and the oil phase were both important in controlling the microsphere size. To fine-tune the GelMA droplet diameter, oil phase flow rate (Q_O) was kept constant at 10 mL h^{-1} while flow rate of GelMA solution (Q_{Aq}) was varied from 100 to 2000 µL h^{-1} such that Q_{Aq}/Q_O ranged from 0.01 to 0.2, resulting in GelMA microsphere droplets with diameters varying between 90 and 230 µm. Monodisperse GelMA microdroplets of 163 µm diameter were generated at Q_{Aq}/Q_O of 0.1 (Figure 2C,D). This size was chosen to balance the requirements that the microsphere size be larger than 60 µm to ensure a sufficient number of encapsulated cells to promote cell contact and proliferation[31] and smaller than 200 µm to allow ready oxygen exchange across the hydrogels for long-term cell survival.[32]

The resultant droplets were subjected to UV radiation (365 nm, 6.9 mW cm^{-2}) for 20 s. The exposure time was optimized for full conversion of the gelation reaction by measuring the elastic modulus of the microspheres using atomic force microscopy (AFM, see Section 50 below for details) at different exposure time of 15, 20, and 25 s. The elastic modulus of the microspheres after 15, 20, and 25 s of light exposure was found to be 9 ± 2, 15 ± 2, and 15 ± 3 kPa, respectively. Twenty seconds was thus selected as the UV time needed to be long enough to allow full conversion (corresponding to the highest elastic modulus) and short enough to ensure high cell viability. The photopolymerized microspheres were subsequently washed in 20% perfluorooctanoate in HFE oil to remove the surfactant and enhance the transfer of the microspheres to a water phase, followed by washing using distilled water at a ratio of 1:1 by volume. The GelMA microspheres were transferred into the water phase due to their hydrophilic nature. The washing step was repeated twice to ensure complete removal of surfactant and any remnant oil. After immersion in water for 24 h, the crosslinked microspheres were shown to have a slightly larger size of 165 µm (Figure 2E,F) due to a small amount of swelling. Complete diffusion of 0.2% rhodamine 6G (Sigma) into the crosslinked microspheres occurred within half an hour. Such fast diffusion suggests ready nutrient and waste exchange across the hydrogels which is thought to improve long-term cell survival.

2.3. Elastic Modulus and Degradation Behavior of GelMA Microspheres

Once formed, the resultant crosslinked GelMA microspheres could easily be injected through a syringe head (**Figure 3**A). The stiffness of the microspheres helped protect the cells from shear forces experienced upon injection or any other mechanical stresses during their use. To evaluate the GelMA microsphere stiffness, their force-displacement behavior was measured with a nanoindentation technique using an AFM (Figure 3B). Using Hertz contact mechanics theory, the elastic modulus was calculated to be 15 ± 2 kPa. To validate the modulus value calculated from nanoindentation, GelMA hydrogels of cylindrical shape were fabricated at the same concentration. From the stress–strain curve generated by compression, the elastic modulus was calculated to be 14 ± 2 kPa, in excellent accord with the value calculated from the nanoindentation measurements.

To assess the ability of these microspheres to deliver time-critical cargo to bone defects, their degradation performance was investigated by mass-loss analysis. To analyze degradation, GelMA microspheres were incubated in 2 U mL^{-1} collagenase solution. The mass loss increased with time, with complete degradation obtained by day 6 (Figure 3C); this suggests that
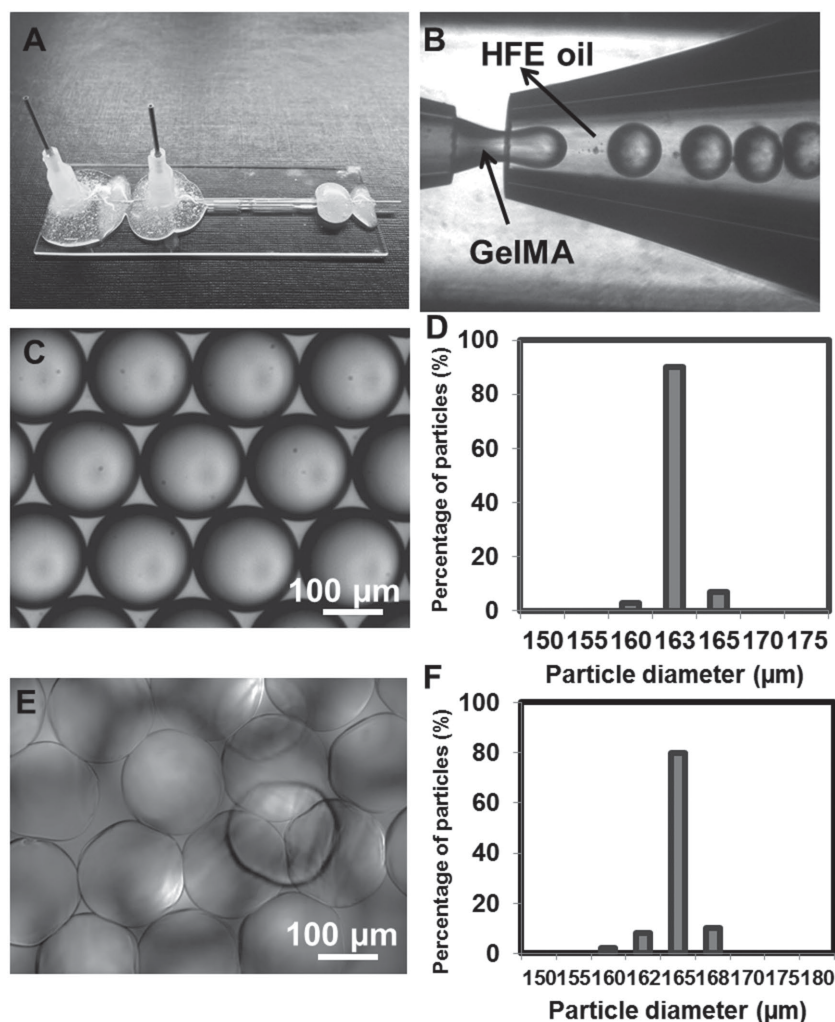
Figure 2. Photocrosslinking-microfluidic fabrication of GelMA microspheres. A). Photograph of the microfluidic device. B). Microscope image of the device generating GelMA droplets. C). Monodisperse GelMA droplets in HFE oil. D). Particle size distribution of GelMA droplets. E) Photopolymerized GelMA microspheres. F) Particle size distribution of crosslinked GelMA microspheres.

GelMA can respond well to the biological environment. Although the in vitro collagenase levels cannot be directly translated to a specific in vivo response due to the complexity of the in vivo environment, similar degradation rates should occur for in vivo environments.[33]

2.4. In Vitro Osteogenic Differentiation of BMSCs Inside GelMA Microspheres

Stem cell survival, spreading, proliferation, and migration are known to significantly affect osteogenic differentiation in vitro and in vivo.[20] To determine the suitability of GelMA microspheres both as in vitro culture platforms and as injectable bone regeneration scaffolds, we first evaluated the BMSC viability by quantifying the live and dead cells encapsulated inside the GelMA microspheres using live/dead assay (**Figure** 4A,B, respectively). Cell viability of >60% was maintained for 7 d, demonstrating innate cyto-compatibility of the GelMA microspheres (Figure 4E). The slight increase in cell viability over time reflects cell proliferation, which occurred relatively readily. The combination of cell proliferation and cell migration from the microspheres, as well as any cell death, resulted in the observed viability ratios. The proliferation that did occur reflected the cell acclimatization to the external environment and subsequent increased cell-cell and cell-matrix signaling, resulting in a self-sufficient microenvironment. We further examined cell adhesion and proliferation using phalloidin/DAPI staining and Picogreen DNA quantification assay, respectively (Figure 4C,D,F).
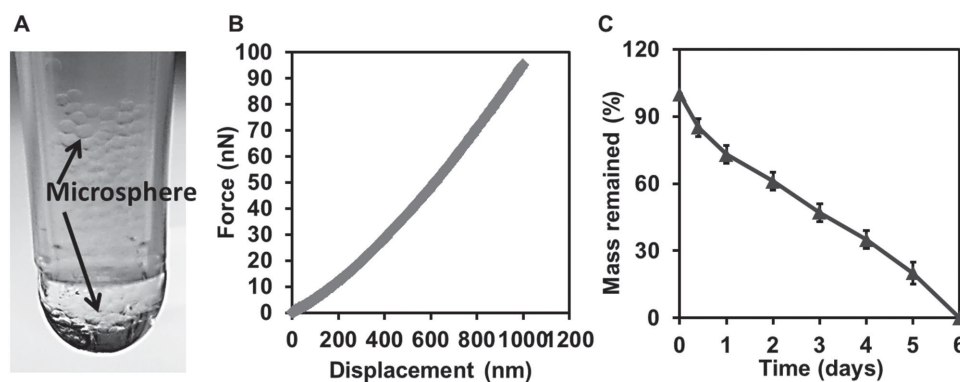
Figure 3. Physical properties of photopolymerized GelMA microspheres. A). Injection of GelMA microsphere through a syringe head with inner diameter of 4.5 mm. B). GelMA microsphere force-displacement curve measured using nanoindentation assisted by atomic force microscopy (AFM). Calculation of elastic modulus is based on Hertz contact mechanics theory. C). Degradation profile of GelMA microspheres incubated with collagenase.

www.MaterialsViews.com

ADVANCED
FUNCTIONAL
MATERIALS
www.afm-journal.de

FULL PAPER
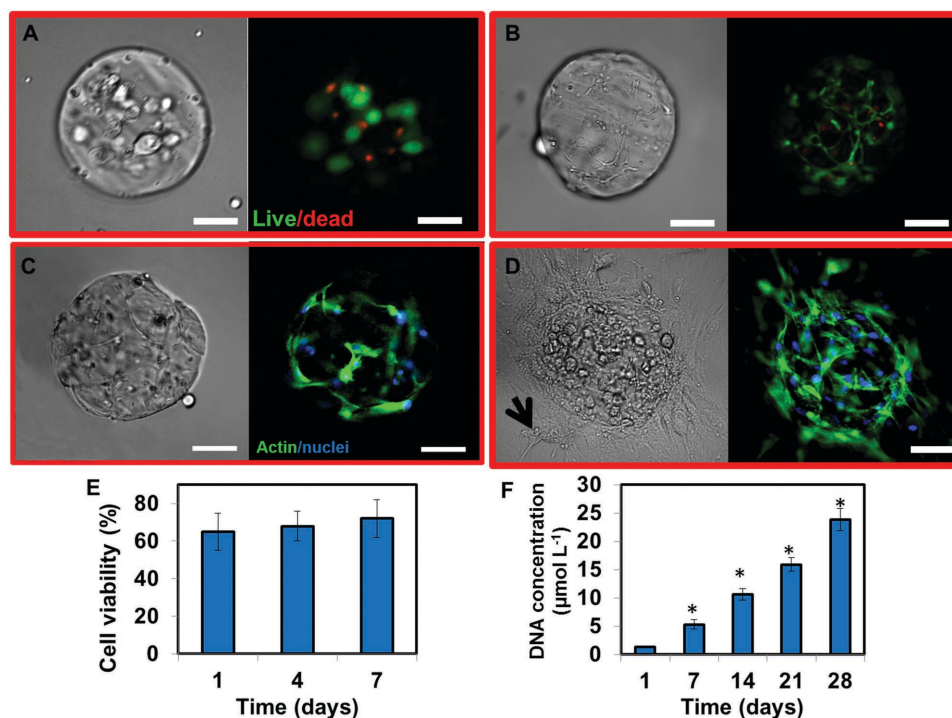
Figure 4. Viability, spreading, and proliferation of BMSCs encapsulated in GelMA microspheres. A,B) Viability of BMSCs encapsulated in GelMA after A) 1 and B) 7 d of culture. Live (green) cells are labeled with calcein AM and dead (red) cells are labeled with ethidium homodimer. C,D) Phalloidin/ DAPI images of BMSCs cultured in GelMA after C) 2 and D) 4 weeks. Phalloidin stains cell filament green and DAPI stains cell nuclei blue. Note that cells migrate significantly outside the microspheres and attach to tissue culture plastic (TCP) at 4 week (arrow). Scale bar = 100 μm. E,F) Quantification of E) cell viability and F) proliferation.

Adherent cells demonstrated a spreading morphology and a characteristic polygonal, polarized shape with projections spreading inside the microspheres (Figure 4C). Moreover, significant cell migration from the interior of the GelMA microspheres to the surface was observed (Figure 4D and **Figure 5**; Figure S2, Supporting Information). After 4 weeks of culture, there was sufficient BMSC migration outside the boundaries of the spheres such that there were large numbers of cells growing on the tissue culture plastic (TCP, Figure 4D see arrow). This is the crucial precondition for the cells' active involvement in the regeneration process. Total DNA content, proportional to cell number, measured during 4 weeks of culture, demonstrated significantly increasing values with time, indicating continuing proliferative capacity of cells grown inside or around GelMA microspheres ($p < 0.05$). Furthermore, viability and morphology of cells released from the GelMA microspheres exhibited the same viability and morphology as that of BMSCs directly seeded onto TCP (Figure 5C,D). Together, these data demonstrated the suitability of GelMA microspheres as delivery vehicles that provide the requisite microenvironment for BMSC survival and proliferation, and the capability to disintegrate over time to release encapsulated cells that can directly and actively participate in the regeneration process.

To investigate the effect of the GelMA microenvironment on the osteogenic differentiation of BMSCs, the activity level of alkaline phosphatase (ALP) and calcium deposition was evaluated. ALP is a key regulator of the early stage differentiation of BMSCs and gradually decreases with further differentiation into osteoblasts.[34] We detected ALP activity relative to the amount of DNA as early as day 1 with minimal levels of approximately 0.002 nM ng^{-1}. Levels peaked around day 7 at 0.025 nM ng^{-1} which was a statistically significant 12.5-fold increase within the space of 1 week (**Figure 6**A, $p < 0.05$). Reduced ALP activities ranging between 0.01 and 0.015 nM ng^{-1} were repeatedly observed from day 14 through to the end of the study on day 28. Previous long-term in vitro and in vivo studies demonstrated that early expression of ALP was associated with deposition of bone type matrix. Subsequent downregulation of ALP with concomitant upregulation of other more advanced osteoblastic markers such as osteopontin and osteocalcin has been shown to be associated with the mineralization of bone.[35] We also investigated calcium deposition by staining with Alizarin red. The percentage of calcium deposits within each GelMA microsphere increased from about 40% after 1 week of culture to almost 70% after 4 weeks; this represented a 1.75-fold increase (Figure 6B,C). The percentage was calculated as the ratio of the number of calcium-bearing microspheres relative to the total number of microspheres. The early reduction of ALP activity and early deposition of calcium may be regulated by the confined 3D environment due to the local accumulation of the stem cell secreted molecules driving differentiation patterns.[14] Both the kinetics of ALP expression and the time-dependent increase in calcium deposition suggest the in vivo osteogenic potential of the BMSC-laden GelMA microspheres.
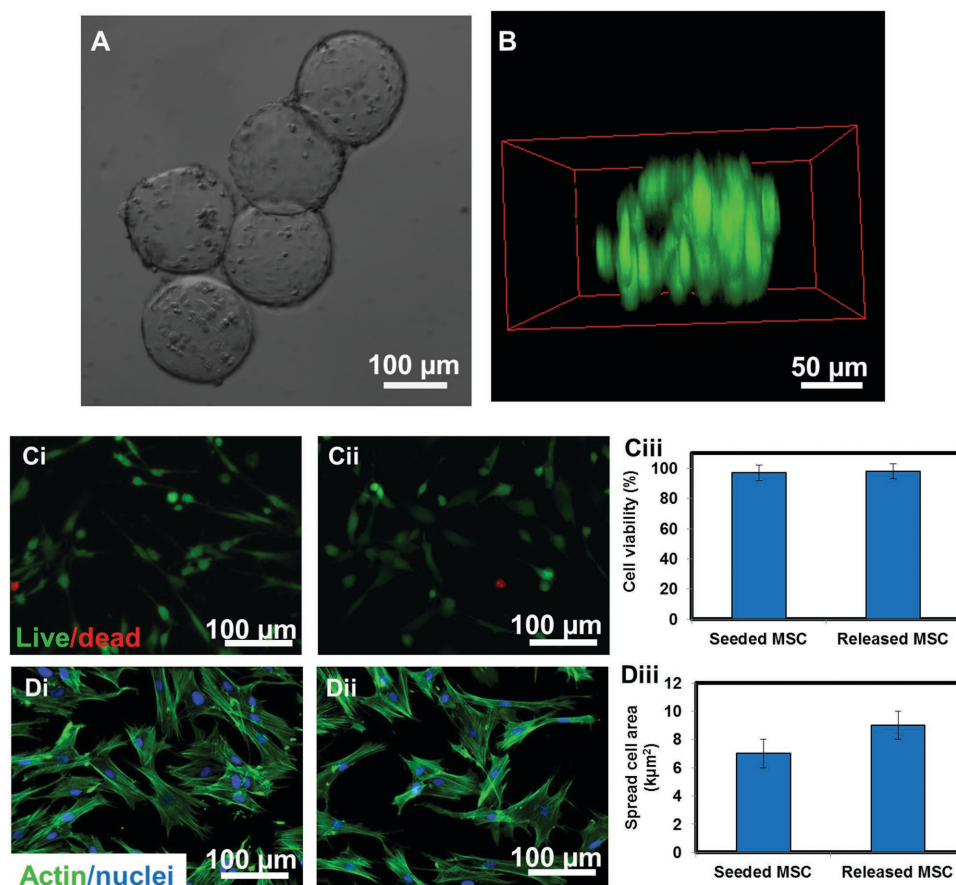
Figure 5. A) Microscope images of BMSCs cultured in GelMA microspheres after 2 weeks. The cells encapsulated inside the microspheres migrate from the microsphere core and adhere on the surface of GelMA microspheres and proliferate over time. B) A 3D reconstructed image of cells in GelMA microsphere. Volume rendering is acquired from 30 optical sections obtained with a laser confocal microscope. Cells are stained green for actin filaments in the cytoplasm. C,D) Representative C) live/dead and D) phalloidin/DAPI stained images of BMSCs directly seeded on TCP (i) and BMSCs released from microspheres (ii). Scale bar = 100 μm. Ciii and Diii represent quantification of (Ciii) cell viability and (Diii) cell area of BMSCs directly seeded on TCP and BMSCs released from microspheres.
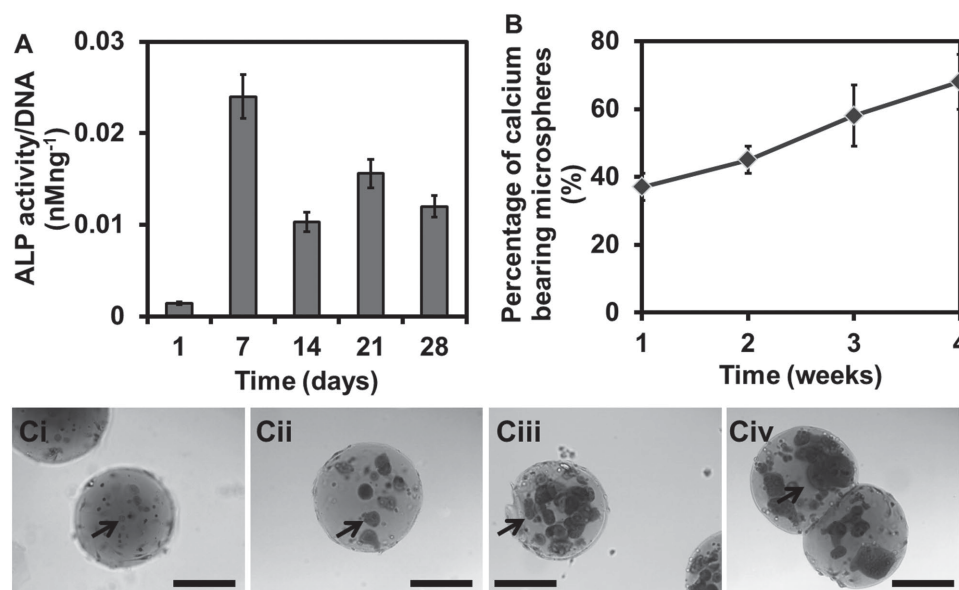
Figure 6. In vitro osteogenesis of BMSCs cultured in GelMA microspheres. A) ALP activity of BMSC cultured in GelMA microspheres. B) Quantification of percentage of calcium bearing microspheres. C) Alizarin red staining of cell-laden microspheres after (i) 1, (ii) 2, (iii) 3, and (iv) 4 weeks of culture. Scale bar = 100 μm.

www.MaterialsViews.com

ADVANCED
FUNCTIONAL
MATERIALS
www.afm-journal.de

FULL PAPER

2.5. In Vitro BMP-2 Release from the GelMA Microspheres

One major advantage of using hydrogels as a cell delivery vehicle is the ready incorporation of growth factors. We chose bone morphogenic protein-2 (BMP-2), an osteogenic growth factor, as it stimulates stem cell differentiation, mineral deposition and osseous tissue development.[36] To determine the release of BMP-2 from the GelMA microspheres, we synthesized microspheres from a solution containing 200 ng mL^{-1} of the prepolymer mix. With an isoelectric point of pH = 5, the GelMA backbone is negatively charged at physiological values of pH[10,37] whereas BMP-2, with an isoelectric point of 7.9, is positively charged.[38] Thus, we hypothesize that there will be an ionic interaction between the crosslinked GelMA network and BMP-2, slowing its release (**Figure 7**A). To test this hypothesis, we measured the BMP-2 encapsulation efficiency and its release from the microspheres as a function of time using a BMP-2 Human ELISA Kit. The encapsulation efficiency was found to be 90%. Regarding the BMP-2 release, there was a minimal burst release of approximately 20% of the initially loaded BMP-2 at time 0, which may be attributable to the weak adsorption of BMP-2 to the GelMA surface resulting in rapid sequestration of BMP-2 from the microspheres.[39] However, subsequent release of BMP-2 was markedly more gradual. By day 5, approximately 80%–90% of BMP-2 was released. The in vitro release of BMP-2 from GelMA microspheres was maintained for approximately 1 week (Figure 7Bi) which is longer than for most hydrogels. This likely reflects the effects of ionic interactions between the GelMA backbone and BMP-2. Such a delayed release behavior of BMP-2 by GelMA microspheres is of significance for the successful repair of bone defects. A plot of BMP-2 release as a function of the square root of time (SQRT) resulted in a linear dependence, as shown in Figure 7 Bii, indicating that BMP-2 release is a result of diffusion.

2.6. Enhanced In Vivo Bone Formation by BMSC and BMP-2 Delivery Using GelMA Microspheres

To evaluate the in vivo therapeutic efficacy of BMSCs, with or without BMP-2, on new bone formation, GelMA microspheres loaded with BMSCs, both with and without BMP-2, were implanted into a rabbit femoral defect. Histological analysis with H&E and VG staining at 4 weeks revealed new bone formation with the largest amount in the GelMA/BMSC/BMP-2 sample, and with incrementally decreasing amounts in the GelMA/BMSC sample, the GelMA sample, and the control sample (**Figure 8**A–C). Bone volumes were derived from area measurements of histology images using the Cavalieri method[40] (Figure 8D). Analysis revealed the most extensive in vivo bone formation, and with that the highest therapeutic efficacy, for the GelMA microspheres delivering both BMSCs and BMP-2 together and the lowest efficacy with GelMA microspheres alone. Similarly, the extent of osteoid, which is the unmineralized or immature portion of the bone matrix, was lower in GelMA microspheres without BMSC or BMP-2 compared to in the GelMA microspheres carrying BMSCs together with BMP-2 (Figure 8E). These results confirmed the synergistic action of the BMP-2 with BMSCs and demonstrated the efficacy of this delivery vehicle for in vivo applications.
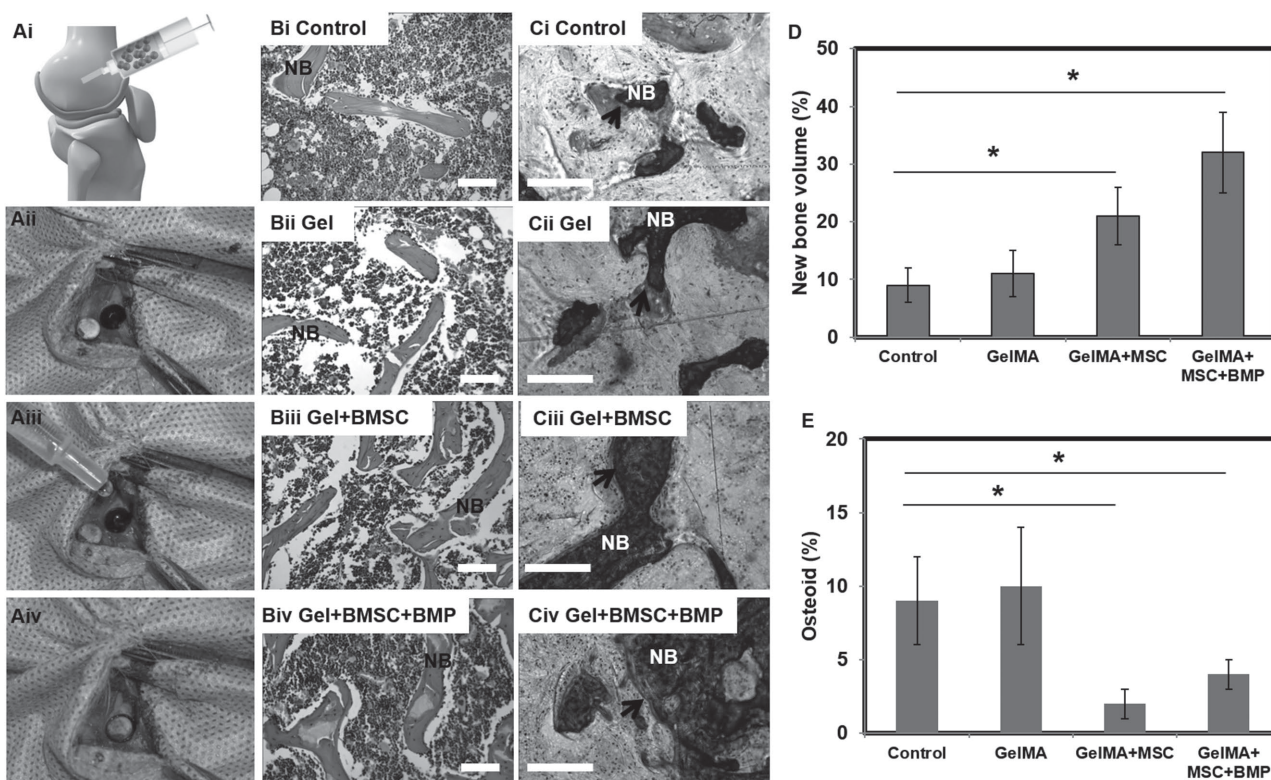
3. Conclusion

Overall, the proposed fabrication strategy using a photocrosslinking microfluidic approach has been deemed both
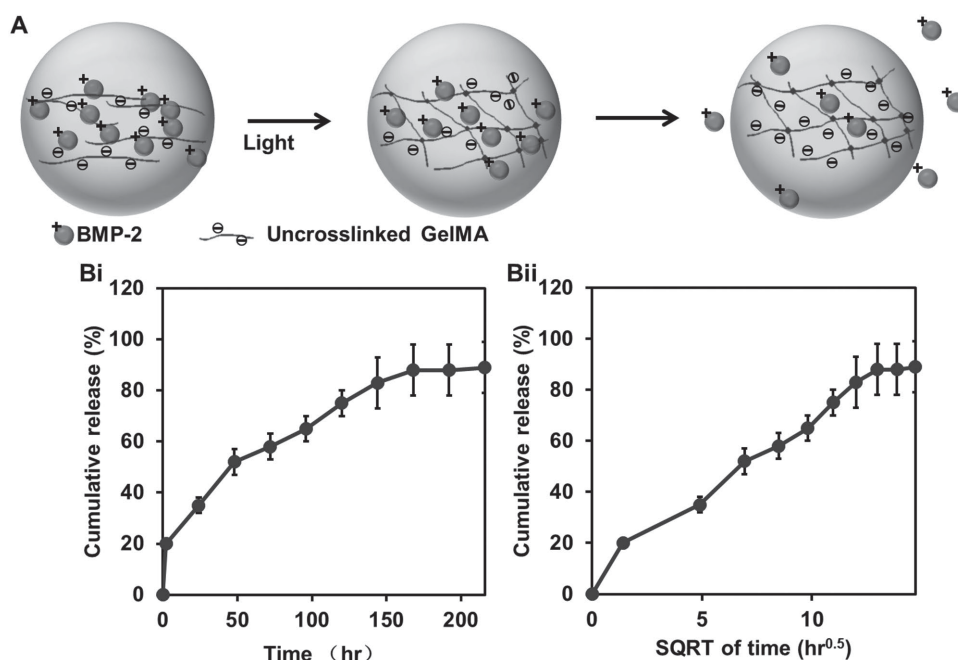
Figure 7. In vitro BMP-2 release from GelMA microspheres. A) Release mechanism. B) Cumulative BMP-2 release with time (Bi) and square root (SQRT) of time (Bii) from GelMA microspheres.

FULL PAPER

Figure 8. Bone defect repair in vivo. A) Operation processes. (Ai) Schematic illustration of rabbit femoral defect model. (Aii) A circular defect is created on the lateral aspect of the distal part of a rabbit femur. (Aiii) Injection of normal saline (control), empty GelMA microspheres (blank) or GelMA microspheres containing BMSC or BMSC + BMP-2 into the wound bed. (Aiv) Closure of the femoral defect using the circular piece of bone originally removed to create the defect. B) Histological sections of nonimplanted (i), implanted GelMA microspheres (ii), BMSC-laden microspheres (iii), and BMSC-laden microspheres containing BMP-2 (iv) in rabbit's femur after implantation for 4 weeks stained using haematoxylin and eosin (H&E) and (C) Van Gieson's Picro–Fuchsine staining. The BMSC-laden GelMA microspheres show more new bone formation than the control after 4 weeks post-surgery. "NB" indicates new bone. Scale bar = 200 μm. D) Histomorphometrical analysis (%) of new bone formation and (E) osteoid (arrows) formation and total area in the defect zone (*$p < 0.05$).

facile and efficient for producing microspheres that provide a BMSC-friendly microenvironment to engineer injectable osteogenic tissue constructs.

In this work, monodisperse droplets containing GelMA gel precursors are produced using a capillary microfluidic device and subsequently expose the drops to UV radiation to photopolymerize the polymer and form GelMA microspheres. Flow rates of both aqueous and oil phases are controlled to tune the microsphere size. BMSCs are encapsulated within the GelMA microspheres to protect the cells and provide a suitable microenvironment for their viability and growth during deposition. Once delivered, BMSCs adhere to and interact with the materials and migrate out of the microspheres, which may benefit graft and host integration at both the cellular and molecular level. More importantly, enhanced bone formation is achieved due to the efficient BMSC encapsulation which ensures long-term survival, proliferation, and migration as well as differentiation into functional osteoblasts. Bone formation is further facilitated by the prolonged release of BMP-2 which is an essential growth factor for the promotion of bone formation and ossification. These BMSC-laden GelMA microspheres have considerable potential as engineered injectable tissue constructs that should have a wide array of applications in regenerative medicine.

4. Experimental Section

Synthesis of GelMA: GelMA was synthesized using the methods previously described.[41] Briefly, using a magnetic stirrer, 10.0 g of type A porcine skin gelatin (Sigma-Aldrich, St. Louis, MO) was dissolved in 100 mL of Dulbecco's phosphate-buffered saline (DPBS) (Invitrogen, San Diego, CA) at 60 °C. 8.0 mL of methacrylic anhydride was added to react with gelatin for 3 h under vigorous stirring at 50 °C. The solution was then subject to a fivefold dilution with warm (40 °C) DPBS to stop the reaction. The solution was dialyzed using a 12–14 kDA cut-off membrane at 40 °C for 1 week to remove any salts and unreacted methacrylic anhydride. Then, the solution was lyophilized for 1 week to obtain a white porous foam, which was stored at −80 °C until further use. The degree of methacrylation was calculated as the ratio of the number of reacted methacrylamide groups to the number of amine groups in unreacted gelatin. Using 1H NMR (Varian Inova 500), these values were obtained by integrating peaks at 7.4 ppm and peaks at 5.5 and 5.7 ppm, which corresponded to aromatic residues of gelatin and to methacrylamide groups, respectively.[42]

Production of Microfluidic Device: The microfluidic device was fabricated on a glass slide which served as a plate. Two cylindrical capillaries which were used as injection and collection tubes were aligned coaxially inside a square capillary preadhered to the glass slide. The injection glass with inner diameter of 0.5 mm and outer diameter of 1.0 mm was tapered using a micropipette puller (P-97, Sutter Co. Ltd., USA) and adjusted by a microforge for inner dispersed phase injection. The diameter of the tapered orifice was approximately 80 μm. The collection tube's inner and outer diameters were the same as those

www.MaterialsViews.com

ADVANCED
FUNCTIONAL
MATERIALS
www.afm-journal.de

FULL PAPER

of the injection tube except for a larger tapered orifice of 160 μm. The inner dimension of the square tube measured 1.0 mm. The space between the circular and square capillaries was used for the injection of the continuous phase. Fluids were injected into the microfluidic device by two microsyringe pumps connected to two gastight microsyringes. The droplets forming in the collection tube were collected with a 50 mL centrifuge tube.

Microsphere Preparation: To prepare GelMA microspheres, 7.5 wt% GelMA solution supplemented with 1.0 wt% 2-hydroxy-4'-(2-hydroxyethoxy)-2-methylpropiophenone (photoinitiator, PI, Sigma-Aldrich, MO) served as the dispersed phase, while HFE7500 oil served as the continuous phase. Both phases were individually injected into the microchannel and the dispersed phase formed monodisperse droplets. The flow rate of water phase and oil phase was adjusted to obtain droplets of sizes smaller than 200 μm. The collected W/O emulsion was polymerized into microspheres upon exposure to 6.9 mW cm^{-2} UV light (365 nm) for 20 s. The light exposure time was optimized to ensure full crosslinking while being as short as possible to minimize cell damage. The size of the resultant microspheres was determined using microscope images and NIH image J software.

Physical Characterization of the GelMA Microspheres—Elastic Modulus Measurement: Force measurements on GelMA microspheres were performed using AFM-assisted nanoindentation, as previously described.[38] An AFM (Asylum Research, Santa Barbara, CA) on a vibration isolation table (Herzan, Laguna Hills, CA) was used for measurements. Using a bright field microscope (Eclipse Ti, Nikon, Melville, NY), a tipless silicon nitride cantilever (MLCT-O10, Bruker, Camarillo, CA, Cantilever E, k = 50 –200 pN nm^{-1}) was located and positioned with a 5.5 μm polystyrene bead (Bangs Labs, Fishers, IN) over the center of each GelMA particle. The cantilever spring constant k was measured to be 110.56 pN nm^{-1} and the probe velocity used was 2 μm s^{-1}. With a 5 nN force trigger, the indentations for typical particles were determined to be about 25 nm. The elastic modulus of each microsphere was determined using IGOR software (Wave metrics, Portland, OR), which applied the Hertzian contact model to the extension force–displacement curves. For result validation, GelMA hydrogels of cylindrical shape were prepared using previously described methods at the same concentration of 7.5 wt%.[28] With a mechanical testing unit (Model 5943, Instron), a uniaxially test was performed on the cylindrical hydrogels and the resultant stress–strain curves were used to calculate elastic modulus, defined as slope values of linear regions from 0% to 10% strain. The elastic modulus was calculated as the average of three measurements.

Physical Characterization of the GelMA Microspheres—Degradation: Samples of 500 μL were incubated at 37 °C with 500 μL of DPBS containing 2 U mL^{-1} of collagenase type II in 1.5 mL Eppendorf tubes for 1 week.[43] Collagenase-containing DPBS was replaced every day to ensure constant enzymatic activity. At predetermined time points, the DPBS was removed from tubes and the samples were washed twice with sterile deionized water, lyophilized, and weighed. The following equation was used to calculate percentage degradation (D)

$$D\% = \frac{W_0 - W_t}{W_0} \times 100\% \qquad (1)$$

where W_0 was the initial sample dry weight and W_t was the dry weight after time t.

Biological Characterization of the Microspheres: Preparation of cell-laden GelMA microspheres was the same as described above. GelMA solution containing BMSCs at density of 10 million mL^{-1} was used. The cell density was optimized for high cell viability. BMSCs were purchased from Lonza (Walkersville, MD) and cells at passage 2–6 were used in this study.

A. Cell culture: The cell-laden GelMA microspheres were washed by the DPBS three times to remove the PI. They were then seeded in a 24 well plate with 100 μL microspheres in each well. Cells were maintained in α-Minimum Essential Medium (α-MEM), supplemented with 15% fetal bovine serum (FBS), 100 units mL^{-1} penicillin, and 100 μg mL^{-1}

streptomycin (Gibco). Cells were maintained in an incubator at 37 °C with 5% CO$_2$.

B. Cell viability: Cell viability was measured after 1 and 7 d of culture to examine the survival rate of BMSCs encapsulated inside GelMA microspheres. At days 1 and 7, cell viability was assessed using calcein AM/ethidium homodimer live/dead assay (Life Technologies, NY) according to the manufacturer's instructions.[42] Live/dead dye solution was prepared by adding 0.5 μL of calcein AM and 2 μL of ethidium homodimer into 1 mL DPBS. Cells were stained by replacing growth medium with 300 μL of live/dead dye solution and incubation in darkness at 37 °C for 15 min. After imaging with Nikon Eclipse Ti-S fluorescence microscope, live and dead cell quantifications were performed using NIH ImageJ software and cell viability was calculated as the ratio of the number of live cells to the total number of cells.

C. Cell spreading: To visualize cell adhesion on samples at weeks 1, 2, 3, and 4, staining of F-actin and cell nuclei was performed using phalloidin (Alexa Fluor 488, Life Technologies, NY) and DAPI (Sigma, St Louis, MO), respectively. Staining was done according to the manufacturer's instructions. Briefly, after washing by 3× PBS, samples were fixed by 4% paraformaldehyde (PFA) for 30 min, permeabilized by 0.1% Triton X-100 for 20 min, and blocked by 1% BSA for 45 min. Cells were incubated in phalloidin solution at dilution 1:40 for 45 min, and then DAPI solution at dilution 1:1000 for 5 min, both at 37 °C. Cells were imaged using Nikon fluorescence microscope and NIH ImageJ software was used to measure both cell number and cell area.[42] Cell migration was imaged using a Zeiss confocal fluorescence microscope. Z-Stacks were collected every 5 μm and prepared using the ImageJ Volume Viewer Plugin (metadata available upon request).

D. Cell proliferation: Proliferation of BMSCs over time was determined by a Picogreen DNA quantification assay. Cells were lysed in 50 μg mL^{-1} proteinase K solution (Sigma, St. Louis, MO) for 2 h and Picogreen DNA quantification assay (Invitrogen, Carlsbad, CA) was used to determine the DNA amount in each culture based on a DNA standard curve.

E. Osteogenic differentiation: To examine osteogenic differentiation capability of BMSCs encapsulated in GelMA microspers, cell-laden microspheres were cultured in OsteoLifeTM osteogenesis medium (Lifeine CellTech, Frederick, MD). After cultures for 1, 2, 3, and 4 weeks, osteogenic differentiation of BMSCs was determined using Alizarin red staining and ALP activity assay.

i. ALP activity measurement: At week 1, 2, 3, and 4, ALP activity was determined using the ALP activity assay (Sigma) according to the manufacturer's protocol. Briefly, the samples were incubated at 37 °C in 500 μL proteinase K solution for 2 h and then centrifuged at 4 °C at 14 000 rpm for 10 min. The ALP activity of the lysate was determined using p-Nitrophenyl phosphate (pNPP). After 60 min incubation at 37 °C, the absorbance of pNPP was measured at 405 nm using a Biotek microplate reader. The ALP activity was normalized for DNA concentration using Quant-iT PicoGreen dsDNA assay. The activity of ALP was calculated as nM ng^{-1} DNA.

ii. Alizarin red staining: Calcifying nodules formed by BMSCs were visualized by Alizarin red (Sigma) staining. Briefly, culture medium was removed and samples were washed twice using DPBS. 4% PFA in DPBS was added to fix the samples for 30 min before washing thrice with distilled water. Then, 500 μL of 2% Alizarin red solution (pH = 4.2) was added to each sample followed by 5-min incubation. Samples were, again, washed with distilled water several times until discoloration was complete. A Nikon microscope with infinicam was used for sample imaging.

F. In Vitro BMP-2 Release Study: To prepare BMP-2 loaded GelMA microspheres containing BMP-2 at concentration of 200 ng mL^{-1}, 2 μL BMP-2 solution (100 μg mL^{-1}, ProSpec) was dissolved in premade 7.5% GelMA solution containing PI. The mixture was then subject to microfluidics/UV exposure for fabrication of BMP-2 encapsulated GelMA microspheres. The resultant GelMA microspheres were washed with distilled water to remove the surfactant. The amount of BMP-2 in the washing liquid was determined using a BMP-2 Human ELISA Kit (see below for details) and the encapsulation efficiency of

BMP-2 in the GelMA microspheres was calculated using the following equation

$$\text{Encapsulation efficiency}(\%) = \frac{\text{Total wt of protein actually encapsulated in microspheres}}{\text{Total wt of protein used in the initial batching}} \times 100\% \quad (2)$$

The *in vitro* release profile of BMP-2 from GelMA microspheres was investigated for a 1 week period. 500 µL GelMA microspheres were placed in Eppendorf tubes containing 500 µL DPBS at 37 °C. At designated time points, the storage solution was removed for fluorescence measurement and replaced with 500 µL fresh DPBS. The concentration of BMP-2 released from GelMA microspheres was determined using a BMP-2 Human ELISA Kit (Abcam, MA) according to the manufacturer's protocol. For this test, 50 µL of the obtained storage solution was added into each well of a 96-well BMP-2 microplate that was previously coated with mouse monoclonal antibodies. After four washes with wash buffer contained in the ELISA kit, 200 µL of BMP-2 conjugate was added into each sample followed by 2 h incubation at room temperature. The samples were washed again and 200 µL of BMP-2 substrate was then added into each well before incubating in the dark at room temperature for 30 min. 50 µL of stop solution was then added into each well and the optical density was determined using a Biotek microplate reader at 485 nm wavelength. The amount of protein released at different time points and the cumulative percentage of protein released relative to the total amount of protein present in each sample were then converted.

In Vivo Bone Regeneration Using BMSC- and BMP-2- Laden GelMA Microspheres—Animal Experiments: Animal experiments were carried out in accordance with the policies of Shanghai Jiao Tong University School of Medicine and the National Institutes of Health. Animal experiments were performed as described previously.[44,45] In brief, 6 month old New Zealand rabbits with a mean body weight of 4.0 ± 0.5 kg were used for the study. Six animals were used per material. Animals were operated under anesthesia of 0.5 mg kg⁻¹ of Acepromazine and 10 mg kg⁻¹ of Ketamine under rigorous aseptic conditions. Using the external lateral knee approach, a cavity of 6 mm diameter and 10 mm depth was made by a drill bit in the femoral condyle parallel to the joint surface. 250 µL GelMA microspheres with or without cells or BMP-2 (45ng) were injected into the cavity and the cortical window was closed before the skin was sutured.

In Vivo Bone Regeneration Using BMSC- and BMP-2- Laden GelMA Microspheres—Histological Preparation and Analysis: The implants were harvested and observed after 4 weeks of implantation. The defects without implantation were considered the controls. All animals were sacrificed by an overdose of thiopental sodium and the femoral condyles were retrieved. The samples were fixed for 24 h in 10% formaldehyde solution buffered with DPBS before overnight rinsing with tap water. Some of the specimens were subjected to decalcification in 10% EDTA buffered with DPBS at room temperature for 1 month. After samples were dehydrated with a graded ethanol series and embedded in paraffin, H&E staining was performed on 4 mm thin sections. Other specimens were embedded in methylmethacrylate without decalcification. The cross-sections were cut to about 50 µm thickness with a Leitz Saw Microtome 1600 (Wetzlar, Germany). Finally, the samples were stained with Van Gieson's Picro–Fuchsine staining (VG stain).[28,44–46]

In Vivo Bone Regeneration Using BMSC- and BMP-2- Laden GelMA Microspheres—Histomorphometric Analysis: All measurements used for histomorphometric analysis were made on two sections from each sample. Different histomorphometric parameters were measured for five fields per VG-stained sections with the help of an eyepiece micrometer (KPL 16, Carl Zeiss, Germany) and an ocular integrator with 100 points (KPL 8, Zeiss, Germany).[44,46] All abbreviations originated from the Histomorphometry Nomenclature Committee of the American Society for Bone and Mineral Research.[47] New bone volume and osteoid tissue volume were derived from area measurement using histology images using the Cavalieri method.[48]

Statistical Analysis: With a sample size of three, data were presented as mean ± standard deviation (SD). Statistical significance was declared if $p < 0.05$ as determined by one-way ANOVA and Scheffe's post hoc test.

Supporting Information

Supporting Information is available from the Wiley Online Library or from the author.

[1] a) T. J. Heino, T. A. Hentunen, *Curr. Stem Cell Res. Ther.* **2008**, *3*, 131; b) R. Siddappa, H. Fernandes, J. Liu, C. van Blitterswijk, J. de Boer, *Curr. Stem Cell Res. Ther.* **2007**, *2*, 209.

[2] M. F. Pittenger, A. M. Mackay, S. C. Beck, R. K. Jaiswal, R. Douglas, J. D. Mosca, M. A. Moorman, D. W. Simonetti, S. Craig, D. R. Marshak, *Science* **1999**, *284*, 143.

[3] N. Dib, H. Khawaja, S. Varner, M. McCarthy, A. Campbell, *J. Cardiovasc. Transl. Res.* **2011**, *4*, 177.

[4] a) J. van Ramshorst, S. Rodrigo, M. Schalij, S. M. A. Beeres, J. Bax, D. Atsma, *J. Cardiovasc. Trans. Res.* **2011**, *4*, 182; b) M. A. Laflamme, K. Y. Chen, A. V. Naumova, V. Muskheli, J. A. Fugate, S. K. Dupras, H. Reinecke, C. Xu, M. Hassanipour, S. Police, C. O'Sullivan, L. Collins, Y. Chen, E. Minami, E. A. Gill, S. Ueno, C. Yuan, J. Gold, C. E. Murry, *Nat. Biotechnol.* **2007**, *25*, 1015; c) R. Palchesko, J. Szymanski, A. Sahu, A. Feinberg, *Cell Mol. Bioeng.* **2014**, *7*, 355.

[5] a) S. MacNeil, *Nature* **2007**, *445*, 874; b) W. L. Hickerson, C. Compton, S. Fletchall, L. R. Smith, *Burns* **1994**, *20*, S52.

[6] W. Hassan, Y. Dong, W. Wang, *Stem Cell Res. Ther.* **2013**, *4*, 32.

[7] S. Gerecht, J. A. Burdick, L. S. Ferreira, S. A. Townsend, R. Langer, G. Vunjak-Novakovic, *Proc. Natl. Acad. Sci. U.S.A.* **2007**, *104*, 11298.

[8] A. Moshaverinia, X. Xu, C. Chen, K. Akiyama, M. L. Snead, S. Shi, *Acta Biomater.* **2013**, *9*, 9343.

[9] B. P. Chan, T. Y. Hui, C. W. Yeung, J. Li, I. Mo, G. C. Chan, *Biomaterials* **2007**, *28*, 4652.

[10] J. W. Nichol, S. T. Koshy, H. Bae, C. M. Hwang, S. Yamanlar, A. Khademhosseini, *Biomaterials* **2010**, *31*, 5536.

[11] T. Kaully, K. Kaufman-Francis, A. Lesman, S. Levenberg, *Tissue Eng. Part B Rev.* **2009**, *15*, 159.

[12] a) R. Chen, S. J. Curran, J. M. Curran, J. A. Hunt, *Biomaterials* **2006**, *27*, 4453; b) M. Serra, C. Correia, R. Malpique, C. Brito, J. Jensen, P. Bjorquist, M. J. Carrondo, P. M. Alves, *PLoS One* **2011**, *6*, e23212; c) F. Gu, B. Amsden, R. Neufeld, *J. Control. Release* **2004**, *96*, 463; d) S. Radin, T. Chen, P. Ducheyne, *Biomaterials* **2009**, *30*, 850.

[13] L. Xiang, S. Wang, M. Yu, *Ann. Plast. Surg.* **2012**, *68*, 229.

Materials
Views
www.MaterialsViews.com

ADVANCED
FUNCTIONAL
MATERIALS
www.afm-journal.de

FULL PAPER

[14] a) G. G. Giobbe, M. Zagallo, M. Riello, E. Serena, G. Masi, L. Barzon, B. Di Camillo, N. Elvassore, *Biotechnol. Bioeng.* **2012**, *109*, 3119; b) R. A. Marklein, J. A. Burdick, *Adv. Mater.* **2010**, *22*, 175; c) J. S. Park, H. N. Yang, S. Y. Jeon, D. G. Woo, K. Na, K.-H. Park, *Biomaterials* **2010**, *31*, 6239.

[15] Y. Man, P. Wang, Y. Guo, L. Xiang, Y. Yang, Y. Qu, P. Gong, L. Deng, *Biomaterials* **2012**, *33*, 8802.

[16] C. L. Franco, J. Price, J. L. West, *Acta Biomater.* **2011**, *7*, 3267.

[17] a) S. A. Abbah, W. W. Lu, D. Chan, K. M. Cheung, W. G. Liu, F. Zhao, Z. Y. Li, J. C. Leong, K. D. Luk, *J. Mater. Sci. Mater. Med.* **2008**, *19*, 2113; b) L. Penolazzi, E. Tavanti, R. Vecchiatini, E. Lambertini, F. Vesce, R. Gambari, S. Mazzitelli, F. Mancuso, G. Luca, C. Nastruzzi, R. Piva, *Tissue Eng. Part C Methods* **2010**, *16*, 141.

[18] a) G. D. Nicodemus, S. J. Bryant, *Tissue Eng. Part B Rev.* **2008**, *14*, 149; b) L. B. Priddy, O. Chaudhuri, H. Y. Stevens, L. Krishnan, B. A. Uhrig, N. J. Willett, R. E. Guldberg, *Acta Biomater.* **2014**, *10*, 4390.

[19] A. W. Lund, J. A. Bush, G. E. Plopper, J. P. Stegemann, *J. Biomed. Mater. Res. B Appl. Biomater.* **2008**, *87*, 213.

[20] G. Crevensten, A. J. Walsh, D. Ananthakrishnan, P. Page, G. M. Wahba, J. C. Lotz, S. Berven, *Ann. Biomed. Eng.* **2004**, *32*, 430.

[21] Z. S. Patel, M. Yamamoto, H. Ueda, Y. Tabata, A. G. Mikos, *Acta Biomater.* **2008**, *4*, 1126.

[22] H.-C. Liang, W.-H. Chang, H.-F. Liang, M.-H. Lee, H.-W. Sung, *J. Appl. Polym. Sci.* **2004**, *91*, 4017.

[23] L. D. Solorio, E. L. Vieregge, C. D. Dhami, P. N. Dang, E. Alsberg, *J. Control. Release* **2012**, *158*, 224.

[24] C. W. Yung, L. Q. Wu, J. A. Tullman, G. F. Payne, W. E. Bentley, T. A. Barbari, *J. Biomed. Mater. Res. A* **2007**, *83*, 1039.

[25] a) H.-C. Liang, W.-H. Chang, K.-J. Lin, H.-W. Sung, *J. Biomed. Mater. Res. A* **2003**, *65A*, 271; b) V. Crescenzi, A. Francescangeli, A. Taglienti, *Biomacromolecules* **2002**, *3*, 1384.

[26] K. Schrobback, T. J. Klein, M. Schuetz, Z. Upton, D. I. Leavesley, J. Malda, *J. Orthop. Res.* **2011**, *29*, 539.

[27] T. P. Lagus, J. F. Edd, *J. Vis. Exp.* **2012**, e4096.

[28] E. Tumarkin, E. Kumacheva, *Chem. Soc. Rev.* **2009**, *38*, 2161.

[29] X. Zhao, Q. Lang, L. Yildirimer, Z. Y. Lin, W. Cui, N. Annabi, K. W. Ng, M. R. Dokmeci, A. M. Ghaemmaghami, A. Khademhosseini, *Adv. Healthcare Mater.* **2015**, *5*, 108.

[30] a) A. D. Griffiths, D. S. Tawfik, *Trends Biotechnol.* **2006**, *24*, 395; b) S. Li, X. Ding, F. Guo, Y. Chen, M. I. Lapsley, S. C. Lin, L. Wang, J. P. McCoy, C. E. Cameron, T. J. *Anal. Chem.* **2013**, *85*, 5468.

[31] R. K. Shah, H. C. Shum, A. C. Rowat, D. Lee, J. J. Agresti, A. S. Utada, L.-Y. Chua, J.-W. Kim, A. Fernandez-Nievesa, C. J. Martineza, D. A. Weitz, *Mater. Today* **2008**, *11*, 18.

[32] E. P. Herrero, E. M. M. D. Valle, M. A. Galán, *Biotechnol. Prog.* **2007**, *23*, 940.

[33] R. K. Jain, P. Au, J. Tam, D. G. Duda, D. Fukumura, *Nat. Biotechnol.* **2005**, *23*, 821.

[34] C. Cha, J. Oh, K. Kim, Y. Qiu, M. Joh, S. R. Shin, X. Wang, G. Camci-Unal, K. T. Wan, R. Liao, A. Khademhosseini, *Biomacromolecules* **2014**, *15*, 283.

[35] J. L. Holloway, H. Ma, R. Rai, J. A. Burdick, *J. Control. Release* **2014**, *191*, 63.

[36] a) L. Malaval, D. Modrowski, A. K. Gupta, J. E. Aubin, *J. Cell Physiol.* **1994**, *158*, 555; b) S. E. Kim, Y. P. Yun, Y. K. Han, D. W. Lee, J. Y. Ohe, B. S. Lee, H. R. Song, K. Park, B. J. Choi, *Carbohydr. Polym.* **2014**, *99*, 700.

[37] a) T. A. Owen, M. Aronow, V. Shalhoub, L. M. Barone, L. Wilming, M. S. Tassinari, M. B. Kennedy, S. Pockwinse, J. B. Lian, G. S. Stein, *J. Cell Physiol.* **1990**, *143*, 420; b) P. Bianco, M. Riminucci, E. Bonucci, J. D. Termine, P. G. Robey, *J. Histochem. Cytochem.* **1993**, *41*, 183.

[38] a) M. Imranul Alam, I. Asahina, K. Ohmamiuda, K. Takahashi, S. Yokota, S. Enomoto, *Biomaterials* **2001**, *22*, 1643; b) T. Noshi, T. Yoshikawa, Y. Dohi, M. Ikeuchi, K. Horiuchi, K. Ichijima, M. Sugimura, K. Yonemasu, H. Ohgushi, *Artif. Organs* **2001**, *25*, 201; c) A. H. Nguyen, J. McKinney, T. Miller, T. Bongiorno, T. C. McDevitt, *Acta Biomater.* **2015**, *13*, 101.

[39] Y. Tabata, *Drug Discov. Today* **2005**, *10*, 1639.

[40] T. Boix, J. Gomez-Morales, J. Torrent-Burgues, A. Monfort, P. Puigdomenech, R. Rodriguez-Clemente, *J. Inorg. Biochem.* **2005**, *99*, 1043.

[41] A. I. Van Den Bulcke, B. Bogdanov, N. De Rooze, E. H. Schacht, M. Cornelissen, H. Berghmans, *Biomacromolecules* **2000**, *1*, 31.

[42] H. Shin, B. D. Olsen, A. Khademhosseini, *Biomaterials* **2012**, *33*, 3143.

[43] M. S. Agren, C. J. Taplin, J. F. Woessner, W. H. Eagistein Jr., P. M. Mertz, *J. Investig. Dermatol.* **1992**, *99*, 709.

[44] J. Wu, X. Zhao, D. Wu, C.-C. Chu, *J. Mater. Chem. B* **2014**, *2*, 6660.

[45] J. X. Lu, A. Gallur, B. Flautre, K. Anselme, M. Descamps, B. Thierry, P. Hardouin, *J. Biomed. Mater. Res.* **1998**, *42*, 357.

[46] S. Liu, F. Jin, K. Lin, J. Lu, J. Sun, J. Chang, K. Dai, C. Fan, *Biomed. Mater.* **2013**, *8*, 025008.

[47] Y. Xie, D. Chopin, C. Morin, P. Hardouin, Z. Zhu, J. Tang, J. Lu, *Biomaterials* **2006**, *27*, 2761.

[48] B. Sahin, M. Emirzeoglu, A. Uzun, L. Incesu, Y. Bek, S. Bilgic, S. Kaplan, *Eur. J. Radiol.* **2003**, *47*, 164.